A MULTI-LEVEL APPROACH FOR MICRO-CRACKED VISCOELASTIC MASONRY

Thi Thu Nga Nguyen, Amna Rekik, Alain Gasser

A MULTI-LEVEL APPROACH FOR MICRO-CRACKED VISCOELASTIC MASONRY

Thi Thu Nga NGUYEN[*1], Amna REKIK[1], Alain Gasser[1]

[1] Univ. Orléans, INSA-CVL, PRISME, EA 4229, F45072, Orléans, France,
thi.nguyen2@etu.univ-orleans.fr;
amna.rekik@univ-orleans.fr;
alain.gasser@univ-orleans.fr

Key words: Homogenization, Viscoelastic, Crack, Masonry

Abstract. This research contributes to the micro-macro modeling of refractory lining present in many reactors (like steel converter or blast furnaces). In order to simplify this study, we consider that the masonry is periodic and that only one component (the mortar) is a microcracked viscoelastic material. The objective is to determine the effective and local behavior of this masonry without crack propagation. This study is based on the coupling between homogenization techniques and brittle fracture mechanics. The relevance of the proposed methodology is assessed through numerical simulations carried out for some examples of masonry available in the literature.

1 INTRODUCTION

In the iron and steel industry, the refractory lining of furnaces is usually made of masonry in which brick joints may be either mortared or dry (without mortar [1]). In most cases, refractory brick linings are installed with mortar because its use to bond the brickwork provides more resistance to thermal shock and a cushion at the brick joint [2]. The temperature inside these structures can reach 1650 degrees which induces non-linear mechanical behavior for the masonry and even leads to the initiation and propagation of cracks in the joints. We know that, a thick mortar tends to decrease the stiffness of structure and increases the likelihood of the possible penetration of process materials into the joints, resulting in the deterioration of the lining. So, the use of thin mortar joint is appropriate and necessary in designing the refractory brick lining system.

Concerning the creep behavior of the mortar which can be induced by severe service conditions, various rheological models namely the Maxwell, Kelvin-Voigt, Ross, Burgers and Modified-Maxwell models may be investigated [3, 4]. There exist several approaches accounting for damage in viscoelastic materials [4, 5]. Indeed, the approach presented in [5] is based on a coupling between continuum damage mechanics and viscoelastic-

1

ity through the generalized Kelvin-Voigt model. Accordingly, a three-dimensional phenomenological model was developed to describe the long-term creep of gypsum rock. The main disadvantage of this model is the difficulty to carry out because the internal damage variable is given by solving a nonlinear equation [5] or due to experimentation [4]. In the work of Nguyen et al. [6], the effective behavior of microcracked linear viscoelastic concrete was derived from a combination of the Griffith's theory and the Eshelby-based homogenization scheme. The safe concrete was assumed to obey to the Burgers model.

In [3], an experimental study was carried in order to investigate the creep of masonry. A number of rheological models are examined to assess their ability to predict the creep of masonry. It was proved that the Modified Maxwell model is the most accurate. According to this result, the Burgers model, namely a Maxwell system connected in series with a Kelvin-Voigt one, and the Modified Maxwell scheme (a parallel combination of the Maxwell model and a spring) models are adopted in this paper to describe the mortar joint's creep. Moreover, in the literature, there are few works investigating the global and local behavior of viscoelastic masonry. For instance, Cecchi and Tralli [7] used the asymptotic homogenization technique to deduce the behavior of a safe (without cracks) viscoelastic periodic masonry cell. The effective behavior of a masonry prism is provided due to periodic homogenization.

In the present study, the coupling between the Griffith's theory and the dilute scheme will be applied to provide the effective behavior of the micro-cracked mortar [6]. In a second step, the expressions proposed in [7] are extended to determine the effective behavior of a periodic microcracked viscoelastic masonry cell.

The paper is organized as follows. The general principle of the proposed approach is presented in section 2. The modified Maxwell and Burgers rheological models are recalled in section 3. The steps allowing the determination of the effective behavior of a microcracked linear viscoelastic mortar are explained in section 4. Section 5 shows the determination of the effective behavior of microcracked viscoelastic masonry. At last, section 6 presents primary results for a loaded masonry panel.

2 GENERAL PRINCIPLE

The objective of this study is to evaluate the effective behavior of masonry subjected to high temperatures inducing nonlinear behavior (viscoelasticity, elasto-(visco-)plasticity, etc.). For the sake of simplicity, it can be assumed that only the mortar is a micro-cracked viscoelastic material [8, 9]. Its behavior (at the safe state) obeys to the Modified Maxwell or Burgers models. The blocks or bricks are assumed to be safe and to have either a rigid or elastic isotropic behavior. In the mortar, the cracks are assumed to be penny-shaped and to have an isotropic distribution. The proposed approach is based on two main steps. Firstly, the homogenization technique is applied in order to assess the effective behavior of the micro-cracked mortar. The results of brittle fracture mechanics (the Griffith's theory) could be useful if we move from the real temporal space to the symbolic one due the Laplace-Carson (LC) transform. In the later space, the apparent behavior of the mortar

is linear elastic. This procedure allows the use of expressions available in the literature for the displacement jump induced by the crack [6]. Assuming again that the displacement jump field depends linearly on the macroscopic stress, it is possible to define an effective linear behavior for the micro-cracked mortar in the symbolic space. To determine the global behavior in the real space time, it is possible to apply the inverse of the LC transform in some simple cases. It is then interesting to approach in the symbolic space, at least in short and long terms, the symbolic effective stiffness (or compliance) by an existing rheological model. For example, if the safe mortar behaves as the Modified Maxwell model, we try to approach the symbolic effective behavior of the corresponding microcracked mortar by the same model. After validation of this approximation at short and long terms, the inversion of the apparent effective stiffness will be straightforward. Therefore, the effective behavior of the micro-cracked viscoelastic mortar could be expressed in the real space time.

In a second step, the global behavior proposed for safe linear viscoelastic periodic masonry cell masonries [7] is extended in this study for similar masonry cell with microcracks.

3   RHEOLOGICAL MODELS FOR SAFE VISCOELASTIC MORTAR

In the literature, several rheological models are proposed for the creep of mortar [3, 4]. In this work, only the Burgers and Modified Maxwell models will be considered.

(a) The Modified Maxwell model   (b) The Burgers model
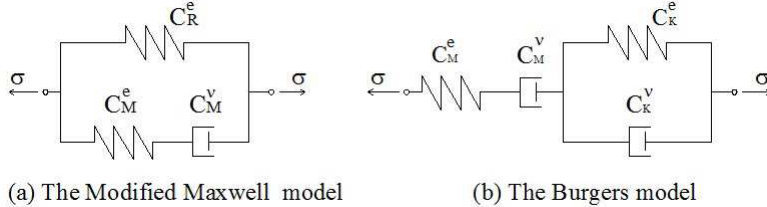
Figure 1: Rheological models for the creep of mortar.

3.1   Modified Maxwell model

The local behavior of the Modified Maxwell model referred to as hereafter by "MM" (fig.1-a) reads:

$$\mathbb{S}_M^v \sigma + \mathbb{S}_M^e \dot{\sigma} = \mathbb{S}_M^v \mathbb{C}_R^e \varepsilon + \left(\mathbb{I} + \mathbb{S}_M^e \mathbb{C}_R^e \right) \dot{\varepsilon} \tag{1}$$

where the stiffness tensor of the spring $\mathbb{C}_R^e = 3k_R \mathbb{J} + 2\mu_R \mathbb{K}$ is added to the elastic $\mathbb{C}_M^e = 3k_M \mathbb{J} + 2\mu_M \mathbb{K}$ and viscoelastic $\mathbb{C}_M^v = \eta_M^s \mathbb{J} + \eta_M^d \mathbb{K}$ stiffnesses of the classical Maxwell model. ε and σ are respectively the strain and stress fields. $\mathbb{S}_\alpha^\beta$ is the compliance fourth-order tensor inverse of $\mathbb{C}_\alpha^\beta$, where the symbol $\alpha = M$ (Maxwell) or R (Spring) and $\beta = h$ (v) for horizontal (vertical) joints. The fourth-order spherical and deviatoric projectors are respectively denoted by: $\mathbb{J} = \mathbf{i} \otimes \mathbf{i}/3$ and $\mathbb{K} = \mathbb{I} - \mathbb{J}$. $\mathbf{i}$ and $\mathbb{I}$ are respectively the

second and fourth-order identity tensors. k_α and μ_α represent the bulk and shear moduli. η_α^s and η_α^d respectively denote the bulk and shear viscosity parameters. In the symbolic space, the constitutive law (1) is given by:

$$\mathbb{S}_M^v \sigma^* + p\mathbb{S}_M^e \sigma^* = \mathbb{S}_M^v \mathbb{C}_R^e \varepsilon^* + p\left(\mathbb{I} + \mathbb{S}_M^e \mathbb{C}_R^e\right)\varepsilon^* \tag{2}$$

where $f^*(p) = p\int_0^\infty f(t)e^{-pt}dt$ (p is a scalar) is the Laplace-Carson transform for all temporal function $f(t)$. The apparent local behavior of the mortar is isotropic linear elastic since the apparent "stress-strain" relation (2) can be written as follows: $\sigma^* = \mathbb{C}^* : \varepsilon^*$. The stiffness tensor $\mathbb{C}^*$ in the symbolic space can be put in the form: $\mathbb{C}^* = 3k^*\mathbb{J} + 2\mu^*\mathbb{K}$ with the following apparent bulk and shear moduli for the safe mortar:

$$k^* = k_R + \frac{1}{\frac{1}{k_M} + \frac{3}{p\eta_M^s}}, \quad \mu^* = \mu_R + \frac{1}{\frac{1}{\mu_M} + \frac{2}{p\eta_M^d}} \tag{3}$$

Under uniaxial compressive loading: $\boldsymbol{\Sigma}^* = \Sigma_{nn}^* \mathbf{n} \otimes \mathbf{n}$ where n is the normal to the crack, the creep function can be deduced from the macroscopic relationship: $\overline{\varepsilon}_{nn}^* = J_{nn}^* \Sigma_{nn}^*$ with $J_{nn}^* = \frac{1}{E^*} = \frac{1}{9k^*} + \frac{1}{3\mu^*}$ and $\overline{\varepsilon}_{nn}^*$ is the apparent normal macroscopic strain. According to equation (3) and after the inversion of the LC transform of J^*, the "real" creep function related to the MM model reads:

$$J_{MM}(t) = \frac{1}{9k_R} + \frac{1}{3\mu_R} - \frac{k_M}{9k_R(k_R + k_M)}e^{-t/\tau_{MM}^s} - \frac{\mu_M}{3\mu_R(\mu_R + \mu_M)}e^{-t/\tau_{MM}^d} \tag{4}$$

where $\tau_{MM}^s = \frac{\eta_M^s(k_R + k_M)}{3k_R k_M}$ and $\tau_{MM}^d = \frac{\eta_M^d(\mu_R + \mu_M)}{2\mu_R \mu_M}$ are the characteristic relaxation times associated respectively to the spherical and deviatoric parts of the creep behavior following the MM model.

3.2 Burgers model

For this model (fig.1-b), the local behavior takes the form:
$$\mathbb{X} : \sigma + \mathbb{Y} : \dot{\sigma} + \mathbb{Z} : \ddot{\sigma} = \mathbb{C}_K^e : \dot{\varepsilon} + \mathbb{C}_K^v : \ddot{\varepsilon} \tag{5}$$

in which the fourth-order tensors $\mathbb{X}$, $\mathbb{Y}$ and $\mathbb{Z}$ are given by: $\mathbb{X} = \mathbb{C}_K^e : \mathbb{S}_M^v$, $\mathbb{Y} = \mathbb{I} + \mathbb{C}_K^e : \mathbb{S}_M^e + \mathbb{C}_K^v : \mathbb{S}_M^v$ and $\mathbb{Z} = \mathbb{C}_K^v : \mathbb{S}_M^e$. Due to the LC transform, the apparent bulk and shear moduli of the mortar without cracks read respectively:

$$\frac{1}{k_{Bu}^*} = \frac{1}{k_M} + \frac{1}{p\eta_M^s/3} + \frac{1}{k_K + p\eta_K^s/3}, \quad \frac{1}{\mu_{Bu}^*} = \frac{1}{\mu_M} + \frac{1}{p\eta_M^d/2} + \frac{1}{\mu_K + p\eta_K^d/2} \tag{6}$$

The real creep function of the Burgers model reads then:

$$J_{Bu}(t) = \frac{1}{9k_M} + \frac{1}{3\mu_M} + \left(\frac{1}{3\eta_M^s} + \frac{2}{3\eta_M^d}\right)t + \frac{1}{9k_K}\left(1 - e^{-t/\tau_K^s}\right) + \frac{1}{3\mu_K}\left(1 - e^{-t/\tau_K^d}\right) \tag{7}$$

where τ_K^s and τ_K^d are the characteristic relaxation times given by: $\tau_K^s = \frac{\eta_K^s}{3k_K}$ and $\tau_K^d = \frac{\eta_K^d}{2\mu_K}$. Note that the Burgers relaxation times are identical to that of the Kelvin-Voigt scheme.

4 EFFECTIVE PROPERTIES OF MICRO-CRACKED VISCOELASTIC MORTAR

4.1 Coupling between the Griffith's theory and linear homogenization technique

As previously mentioned, we assume that the mortar is a linear viscoelastic material occupying the area Ω and containing a parallel network of penny-shaped cracks. During the loading time interval, it is assumed that the displacement $u(x,t)$ prescribed on the boundary of the area $\partial\Omega$ is related to the macroscopic strain $\overline{\varepsilon}(t)$ as follows : $u(x,t) = \overline{\varepsilon}(t).x$. According to the principle of macro-homogeneity, the macroscopic strain is deduced from the average of the local strain $\varepsilon(t)$ in the safe matrix corrected by the strain induced by the presence of micro-cracks as shown in the following:

$$\overline{\varepsilon} = \frac{1}{V}\left(\int_{\Omega_s}\varepsilon dV + \sum_i \int_{C_i}[u]_i \otimes^s n_i dS\right) \tag{8}$$

where Ω_s is the domain occupied by the safe material (without cracks), V is the volume of Ω and $a \otimes^s b = \frac{a\otimes b + b\otimes a}{2}$ for the vectors a and b. C_i and n_i denote respectively the area of the crack i and the normal vector to the plane of this crack. $[u]_i$ denotes the displacement jump at the lips of crack i. Due to the Laplace-Carson (LC) transform, the equation (8) can be rewritten as follows:

$$\overline{\varepsilon}^* = \frac{1}{V}\left(\int_{\Omega_s}\varepsilon^* dV + \sum_i \int_{C_i}[u]_i^* \otimes^s n_i dS\right) \tag{9}$$

The objective is to establish the relationship between the apparent macroscopic strain $\overline{\varepsilon}^*$ and stress $\mathbf{\Sigma}^*$. Since the local behavior of the mortar without cracks reads $\sigma^* = C_s^* : \varepsilon^*$ (see section 3), the equation (9) gives:

$$\overline{\varepsilon}^* = C_s^{*-1} : \mathbf{\Sigma}^* + \frac{1}{V}\left(\sum_i \int_{C_i}[u]_i^* \otimes^s n_i dS\right) \tag{10}$$

where C_s denotes the stiffness tensor of the safe mortar. Note that the relation between the displacement jump $[u]_i^*$ and the applied symbolic stress $\mathbf{\Sigma}^*$ can be estimated by one of the available linear homogenization models such as the dilute scheme, the Mori-Tanaka model, etc. [10]. The coupling between the dilute scheme and Griffith's theory provides the following expressions for the normal and tangential jumps of the displacement field at the crack, respectively:

$$[u_n]^* = \frac{4(1-\nu_s^*)}{\pi}\frac{\Sigma^*}{\mu_s^*}\sqrt{l^2-\rho^2} \quad \text{(11a)} \qquad [u_t]^* = \frac{4(1-\nu_s^*)}{\pi(2-\nu_s^*)}\frac{\Sigma^*}{\mu_s^*}\sqrt{l^2-\rho^2} \quad \text{(11b)}$$

where ν_s^* and μ_s^* are respectively the apparent Poisson's ratio and shear modulus of the safe mortar. l and ρ denote respectively the penny-shaped crack's half length and the distance to the axis of symmetry of the crack.

4.2 Effective properties of the cracked viscoelastic mortar

4.2.1 In the symbolic space

Similarly to the effective strain in the matrix, the displacement jumps (11a) and (11b) depend linearly on the apparent macroscopic stress Σ^*. Therefore, it is possible to re-write the equation (10) as follows: $\bar{\varepsilon}^* = \widetilde{\mathbb{C}}_c^{*^{-1}} : \Sigma^*$ where $\widetilde{\mathbb{C}}_c^*$ is the apparent effective stiffness tensor of the micro-cracked viscoelastic mortar. As the matrix is isotropic and cracks are parallel, the apparent stiffness $\widetilde{\mathbb{C}}_c^*$ is isotropic and reads: $\widetilde{\mathbb{C}}_c^* = 3\tilde{k}_c^* \mathbb{J} + 2\tilde{\mu}_c^* \mathbb{K}$. $\tilde{k}_c^*$ and $\tilde{\mu}_c^*$ are the apparent effective bulk and shear moduli, respectively given by:

$$\frac{1}{\tilde{k}_c^*} = \frac{1 + d_c Q^*}{k_s^*} \qquad (12a) \qquad\qquad \frac{1}{\tilde{\mu}_c^*} = \frac{1 + d_c M^*}{\mu_s^*} \qquad (12b)$$

with: $Q^* = \frac{16}{9}\frac{1-\nu_s^{*2}}{1-2\nu_s^*}$, $M^* = \frac{32}{45}\frac{(1-\nu_s^*)(5-\nu_s^*)}{1-2\nu_s^*}$ and $d_c = Nl^3$ is the damage parameter or crack density parameter where N is the number of cracks per unit of volume. It is noted that k_c^* is deduced from the combination of equations (10) and (11a) leading to:

$$\bar{\varepsilon}^* = C_s^{*-1} : \Sigma^* \mathbf{i} + \frac{8d_c}{9}\frac{\Sigma^*(1-\nu_s^*)}{\mu_s^*}\mathbf{i} \qquad (13)$$

where the macroscopic loading is purely spherical i.e. $\boldsymbol{\Sigma}^* = \Sigma_{ii}^* \mathbf{i}$ ($i = 1, 2, 3$) and knowing that $trace(\bar{\varepsilon}^*) = \bar{\varepsilon}_{ii}^*/3 = \Sigma^*/\tilde{k}_c^*$.

Under a deviatoric macroscopic loading $\boldsymbol{\Sigma}^* = \Sigma^*(e_1 \otimes e_1 - e_3 \otimes e_3)$ in a Cartesian coordinate system (e_1, e_2, e_3) (e_1 and e_3 are respectively parallel and normal to the crack's plane), the linear relation between the crack displacement jumps (11a), (11b) and the apparent macroscopic stress allows to rewrite the apparent macroscopic strain (10) as follows: $\bar{\varepsilon}^* = \Sigma^*/2\tilde{\mu}_c^* = \Sigma^*(1 + d_c M^*)/2\mu_s^*$ and hence to deduce the apparent effective shear moduli given above (12b) (for more details, see [6]).

4.2.2 In the real space time

In order to move from the symbolic space to the temporal real one, it is useful to approximate the apparent effective moduli (12a), (12b) with expressions associated to existent or predefined rheological models. Accordingly, the inverse LC transform can be determined analytically without any approximation related to a numerical inversion scheme [11]. For concrete damaged material, the work [6] identified the best approximation of the apparent stiffness tensor $\widetilde{\mathbb{C}}_{Bu}^*(p, d_c)$ due to the coupling between the homogenization techniques and the mechanics of brittle fracture leading to a creep behavior which follows also a Burgers model at least at short ($t \to 0$) and long ($t \to \infty$) terms. In this study, a similar approach is followed to a mortar which obeys to the MM model at the safe state. Accordingly, the bulk and shear moduli of micro-cracked viscoelastic mortar in the symbolic space have the following expressions:

$$\tilde{k}^*_{MM}(p, d_c) = k_R(d_c) + \frac{1}{\frac{1}{k_M(d_c)} + \frac{3}{p\eta^s_M(d_c)}}$$
$$\tilde{\mu}^*_{MM}(p, d_c) = \mu_R(d_c) + \frac{1}{\frac{1}{\mu_M(d_c)} + \frac{2}{p\eta^d_M(d_c)}} \tag{14}$$

For microcracked mortar with a matrix which the behavior follows the Burgers model, the apparent effective moduli can be well approximated by:

$$\frac{1}{\tilde{k}^*_{Bu}(p, d_c)} = \frac{1}{k_M(d_c)} + \frac{3}{p\eta^s_M(d_c)} + \frac{1}{k_K(d_c) + p\eta^s_K(d_c)/3}$$
$$\frac{1}{\tilde{\mu}^*_{Bu}(p, d_c)} = \frac{1}{\mu_M(d_c)} + \frac{2}{p\eta^d_M(d_c)} + \frac{1}{\mu_K(d_c) + p\eta^d_K(d_c)/2} \tag{15}$$

Using the correspondance theorems on the initial and final values $\lim_{p \to 0} f^*(p) = \lim_{t \to \infty} f(t)$ and $\lim_{p \to \infty} f^*(p) = \lim_{t \to 0} f(t)$, the viscosity parameters of the damaged mortar are determined by the developments in series of the estimated apparent moduli (12a), (12b) to the first-order at p (at $1/p$) when $p \to 0$ ($p \to \infty$). The resulting damaged stiffness and viscosity parameters related to the MM model read:

$$\frac{1}{k_R(d_c)} = \frac{1 + Q^e_M d_c}{k_R}, \quad \frac{1}{k_M(d_c)} = \frac{1 + Q^e_M d_c}{k_R + k_M - k_R(1 + Q^e_M d_c)/(1 + Q^v_M d_c)},$$
$$\frac{1}{\mu_R(d_c)} = \frac{1 + M^v_M d_c}{\mu_R}, \quad \frac{1}{\mu_M(d_c)} = \frac{1 + M^e_M d_c}{\mu_R + \mu_M - \mu_R(1 + M^e_M d_c)/(1 + M^v_M d_c)},$$
$$\frac{1}{\eta^s_M(d_c)} = \frac{(1 + Q^v_M d_c)^2}{\eta^s_M + \eta^s_M Q^v_M d_c - 3k_R Q^0_1 d_c}, \quad \frac{1}{\eta^d_M(d_c)} = \frac{(1 + M^v_M d_c)^2}{\eta^d_M(1 + M^v_M d_c) - 2d_c \mu_R M^0_1} \tag{16}$$

For the expressions of Q^β_α and M^β_α, see Appendix A. The eight damaged stiffness and viscosity parameters of the Burgers model are given by (see also Appendix B):

$$\frac{1}{k_M(d_c)} = \frac{1 + Q^e_M d_c}{k_M}, \quad \frac{1}{\mu_M(d_c)} = \frac{1 + M^e_M d_c}{\mu_M}, \quad \frac{1}{\eta^s_M(d_c)} = \frac{1 + Q^v_M d_c}{\eta^s_M}, \quad \frac{1}{\eta^d_M(d_c)} = \frac{1 + M^v_M d_c}{\eta^d_M}$$
$$\frac{1}{k_K(d_c)} = \frac{1 + Q^e_K d_c}{k_K}, \quad \frac{1}{\mu_K(d_c)} = \frac{1 + M^e_K d_c}{\mu_K}, \quad \frac{1}{\eta^s_K(d_c)} = \frac{1 + Q^v_K d_c}{\eta^s_K}, \quad \frac{1}{\eta^d_K(d_c)} = \frac{1 + M^v_K d_c}{\eta^d_K} \tag{17}$$

Accordingly, the real creep functions of the microcracked viscoelastic mortar read:

$$\widetilde{J}_{MM}(t, d_c) = \frac{1}{9k_R(d_c)} + \frac{1}{3\mu_R(d_c)} - \frac{k_M(d_c)}{9k_R(d_c)\left(k_R(d_c) + k_M(d_c)\right)}e^{-t/\tau^s_M(d_c)}$$
$$- \frac{\mu_M(d_c)}{3\mu_R(d_c)\left(\mu_R(d_c) + \mu_M(d_c)\right)}e^{-t/\tau^d_M(d_c)} \tag{18}$$

$$
\tilde{J}_{Bu}(t, d_c) = \frac{1}{9k_M(d_c)} + \frac{1}{3\mu_M(d_c)} + \left(\frac{1}{3\eta_M^s(d_c)} + \frac{2}{3\eta_M^d(d_c)} \right) t
$$
$$
+ \frac{1}{9k_M(d_c)} \left(1 - e^{-t/\tau_K^s(d_c)} \right) + \frac{1}{3\mu_M(d_c)} \left(1 - e^{-t/\tau_K^d(d_c)} \right) \qquad (19)
$$

respectively for the MM and Burgers models. Actually, the characteristic relaxation times are given by: $\tau_M^s(d_c) = \frac{\eta_M^s(d_c)(k_R(d_c)+k_M(d_c))}{3k_R(d_c)k_M(d_c)}$, $\tau_M^d(d_c) = \frac{\eta_M^d(d_c)(\mu_R(d_c)+\mu_M(d_c))}{2\mu_R(d_c)\mu_M(d_c)}$ for the MM model and $\tau_K^s(d_c) = \frac{\eta_K^s(d_c)}{3k_K(d_c)}$, $\tau_K^d(d_c) = \frac{\eta_K^d(d_c)}{2\mu_K(d_c)}$ for the Burgers scheme.

5 PERIODIC HOMOGENIZATION OF MASONRY WITH VISCOELASTIC CRACKED MORTAR

In this part and for the sake of shortness, we present only a 2D application of the proposed approach described above. We treat the case of a masonry panel studied by Cecchi et Tralli [7] subjected to three distributed loads at the top and two lateral edges and to a concentrated load F at the top as shown in Fig.2-b. Bricks are assumed to be rigid. The mortar inside the joints is assumed to be microcracked with a matrix which obeys to linear viscoelastic behavior. As the arrangement of the bricks is regular, the effective behavior of the panel is assumed to be well estimated by that of a periodic cell (see Figure 2-a). The panel can then be modeled as an homogeneous equivalent material (HEM) which mechanical properties are given by the effective stiffness $\tilde{C}_c$. The material data used to compute this problem are provided in Table 1.
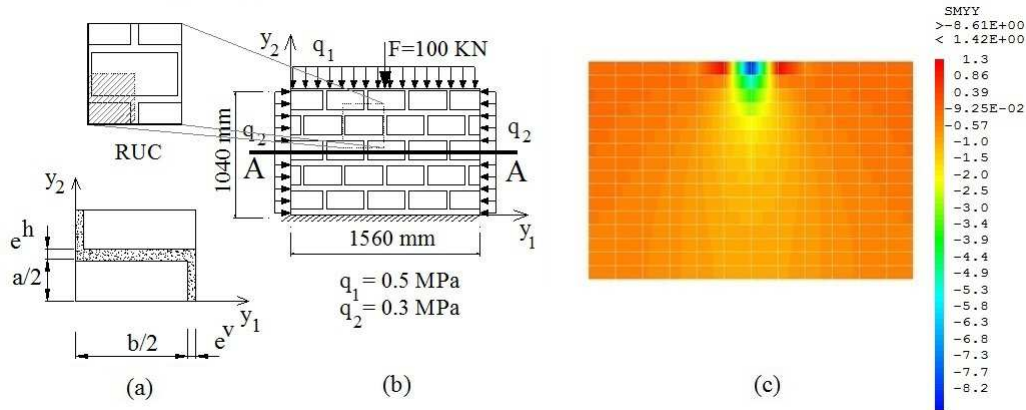
Figure 2: Masonry panel: (a) Representative periodic unit cell and its quarter. (b) Compression test applied to the wall. (c) Snapshot of the stress field σ_{22} (MPa) predicted by the MM and Burgers models at $t = 100$ (s).

The geometric characteristics of the masonry are: $e^h = e^v = 1mm$ - the thickness of bed and head joints. $a = 55mm$, $b = 250mm$ are the block height and length, respectively.

The Poisson's ratio of the mortar is $\nu^m = 0.2$. In [7], the safe mortar was modeled as an interface with constitutive functions of the interface: $K_h' = \frac{E_h^m \Phi_h^m(t)}{(1+\nu_h^m)(1-2\nu_h^m)}$, $K_v' = \frac{E_v^m \Phi_v^m(t)}{(1+\nu_v^m)(1-2\nu_v^m)}$, $K_h'' = \frac{E_h^m \Phi_h^m(t)}{2(1+\nu_h^m)}$, $K_v'' = \frac{E_v^m \Phi_v^m(t)}{2(1+\nu_v^m)}$, in which E_γ^m and ν_γ^m respectively denote the Young's moduli and Poisson's ratios where $\gamma = h$ ou v for horizontal and vertical mortar joints, respectively. $\Phi_\gamma^m(t)$ are the viscous functions of the mortar given by $J_m^{-1}(t) = E^m(t_0)\Phi^m(t)$ where $E^m(t_0)$ is the Young's modulus of the mortar at the initial instant t_0. The effective stiffness components of the masonry periodic cell with mortar in its safe state (without cracks) read [7]:

$$\tilde{C}_{1111} = \frac{\left(4K_v' \dfrac{e^h}{a+e^h} + \dfrac{b+e^v}{a+e^h}K_h'' \dfrac{e^v}{a+e^h}\right)}{4\dfrac{e^h}{a+e^h}\dfrac{e^v}{b+e^v}}, \quad \tilde{C}_{2222} = \frac{K_h'}{\dfrac{e^h}{a+e^h}}, \quad \tilde{C}_{1122} = 0,$$

$$\tilde{C}_{1212} = \frac{K_h''\left(K_h'\dfrac{e^v}{b+e^v} + 4\dfrac{a+e^h}{b+e^v}K_h''\dfrac{e^h}{b+e^v}\right)}{\dfrac{e^h}{a+e^h}\left(K_h'\dfrac{e^v}{b+e^v} + 4\dfrac{a+e^h}{b+e^v}K_h''\dfrac{e^h}{b+e^v} + 4\left(\dfrac{a+e^h}{b+e^v}\right)^2 K_v''\dfrac{e^v}{b+e^v}\right)} \tag{20}$$

For masonry panel with microcracked viscoelastic mortar, the constitutive functions of the interface: $K_h' = \frac{E_h^m(d_c)\Phi_h^m(t,d_c)}{(1+\nu_h^m)(1-2\nu_h^m)}$, $K_v' = \frac{E_v^m(d_c)\Phi_v^m(t,d_c)}{(1+\nu_v^m)(1-2\nu_v^m)}$, $K_h'' = \frac{E_h^m(d_c)\Phi_h^m(t,d_c)}{2(1+\nu_h^m)}$, $K_v'' = \frac{E_v^m(d_c)\Phi_v^m(t,d_c)}{2(1+\nu_v^m)}$ actually account also for the damage parameter d_c. $E_h^m(d_c) = \widetilde{J}_m^{-1}(t_0, d_c)$ at $t_0 = 0$ and $\Phi_h^m(t,d_c) = \widetilde{J}_m^{-1}(t,d_c)/E_h^m(d_c)$ $(t > t_0)$. It is recalled that the creep function $J_m^{-1}(t, d_c)$ is determined by (18) for the MM model and (19) for the Burgers scheme. The modulus $E_h^m(d_c)$ can be rewritten as follows: $\frac{1}{E_h^m(d_c)} = \frac{1}{9(k_M(d_c)+k_R(d_c))} + \frac{1}{3(\mu_M(d_c)+\mu_R(d_c))}$ for the MM and $\frac{1}{E_h^m(d_c)} = \frac{1}{9k_M(d_c)} + \frac{1}{3\mu_M(d_c)}$ for the Burgers models. The effective properties of the periodic cell with materials data given in Table 1 are provided in Table 2 for the safe $(d_c = 0)$ and microcracked $(d_c = 0.3)$ states at two times $(t = 0$ and $t = 100$ days). The engineering constants $\tilde{E}_{11}$, $\tilde{E}_{22}$, $\tilde{\nu}_{12}$, $\tilde{\nu}_{21}$ and $\tilde{G}_{12}$ are provided by the following global "stress-strain" relation: $\bar{\varepsilon}_{ij} = \tilde{C}_{ijkl}^{-1}\bar{\sigma}_{kl} = \begin{pmatrix} 1/\tilde{E}_{11} & -\tilde{\nu}_{12}/\tilde{E}_{11} & 0 \\ -\tilde{\nu}_{21}/\tilde{E}_{22} & 1/\tilde{E}_{22} & 0 \\ 0 & 0 & 1/\tilde{G}_{12} \end{pmatrix}\bar{\sigma}_{kl}$.

Table 1: Elastic and viscous moduli of the considered mortar [12].

Elastic or viscous parts	$k(MPa)$	$\mu(MPa)$	$\eta^s(MPa.s)$	$\eta^d(MPa.s)$
Maxwell	576.67	526.52	$17.18\ 10^8$	$26.52\ 10^6$
Kelvin	714.28	652.17	$65.20\ 10^6$	$2.16\ 10^6$
Spring	714.28	652.17		

Under plane stress assumption, when t exceeds 100 days, the effective stiffness predicted by the Burgers model goes to zero whereas that of the MM model leads to a finite asymptotic limit (see table 2). Figure 2-c shows a heterogeneous symmetric stress local

Table 2: Effective moduli for masonry periodic cell with (safe ($dc = 0$) or damaged ($dc = 0.3$)) linear viscoelastic mortar.

Rheological models	States	*times*	$\widetilde{E}_{11}(GPa)$	$\widetilde{E}_{22}(GPa)$	$\widetilde{G}_{12}(GPa)$
Burgers	Safe	0	564.083	94.188	26.985
		100s	542.372	90.563	25.946
		100days	2114	0.353	0.101
		1000days	0.213	0.036	0.010
	Micro-cracked	0	478.274	79.860	22.880
		100s	459.890	76.791	22.000
		100days	1.833	0.306	0.088
		1000days	0.184	0.031	0.009
MM	Safe	0	1263	210.855	60.410
		100s	1261	210.566	60.327
		100days	699.288	116.765	33.453
		1000days	698.696	116.666	33.425
	Micro-cracked	0	820.924	137.075	39.272
		100s	1070	178.779	51.220
		100days	592.664	98.961	28.352
		1000days	592.409	98.918	28.340

field σ_{yy} with compression for almost all the area of the wall. Small symmetric zones of tension are also observed not so far from the point of application of the concentrated load F.

6   CONCLUSIONS

In this study, the effective behavior of a 2D periodic masonry with a micro-cracked viscoelastic mortar and rigid bricks is firstly provided using the coupling between homogenization techniques and the Griffith's theory. The Burgers and MM models predict local stress exceeding the compressive strength of the considered mortar (around 3.7 MPa [12]) almost throughout the wall except around the zone of application of the concentrated load. This study assumes no interaction between cracks as it is the case of the dilute scheme. Future work will focus on masonry problems with crack propagation and linear homogenization models accounting for interaction between the cracks.

REFERENCES

[1] Andreev, K., Sinnema, S., Rekik, A., Allaoui S., Blond E. and Gasser A. Compressive behaviour of dry joints in refractory ceramic masonry. *Construction and Building Materials.*(2012) **34**: 402–408.

[2] Schacht, Ch. Refractory linings: thermo-mechanical design and applications. *New York: Marcel Dekker Inc.* (1995).

[3] Choi, K.K., Lissel, S.L. and Mahmoud, M.R.T. Rheological modelling of masonry creep. *Canadian Journal of Civil Engineering.*(2007) **34**: 1506–1517.

[4] Ignoul, S., Schueremans, L., Tack, J., Swinnen, L., Feytons, S., Binda, L., Gemert, D.V. and Balen, K.V. Creep behavior of masonry structures - failure prediction

based on a rheological model and laboratory tests. *Structural Analysis of Historical Constructions*, (2007), Conference, New Delhi.

[5] Nedjar, B. and Le Roy, R. An approach to the modeling of viscoelastic damage. Application to the long-term creep of gypsum rock materials. *International Journal for Numerical and Analytical Methods in Geomechanics.* (2013) **37**: 1066–1078.

[6] Nguyen, S.T. and Dormieux, L. A Burger model for the effective behavior of a microcracked viscoelastic solid. *International Journal of Damage Mechanics.*(2011) **20**: 1116–1129.

[7] Cecchi, A. and Tralli, A. A homogenized viscoelastic model for masonry structures. *International Journal of Solids and Structures.* (2012)**49**: 1485–1496.

[8] Sacco, E. A nonlinear homogenization procedure for periodic masonry. *European Journal of Mechanics - A/Solids.*(2009) **28**: :209–222.

[9] Luciano, R. and Sacco, E. Homogenization technique and damage model for old masonry material. *International Journal of Solids and Structures.* (1997) **24**: 3191–3208.

[10] Bornert, M., Bretheau, T. and Gilormini, P. Homogénéisation en mécanique des matériaux, Tome 1 : Matériaux aléatoires élastiques et milieux périodiques. *Hermes science.* (2001).

[11] Rekik, A. and Brenner, R. Optimization of the collocation inversion method for the linear viscoelastic homogenization. *Mechanics Research Communications.* (2011) **38**: 305–308.

[12] Verstrynge, E., Schueremans,L. and Dionys, D.V. Time-dependent mechanical behavior of lime-mortar masonry. *Materials and Structures.* (2011) **44**: 29–42.

Appendix A - Modified Maxwell model

The idea to identify the best approximation of the apparent stiffness tensor of micro-cracked mortar in the class of the same model is to satisfy the series expansions of (12a), (12b) and (14) to the first order at $p = 0$ and $p = \infty$. The series expansion of (14) in the vicinity of $p = 0$ and $p = \infty$ respectively read:

$$\frac{1}{\widetilde{k}^*_{MM}(p, d_c)}\bigg|_{p=0} = \frac{1}{k_R(d_c)} + \theta(p), \quad \frac{1}{\widetilde{k}^*_{MM}(p, d_c)}\bigg|_{p=\infty} = \frac{1}{k_R(d_c) + k_M(d_c)} + \theta(1/p^2), \tag{21}$$

$$\frac{1 + d_c M^*}{\mu^*}\bigg|_{p=0} = \frac{1 + d_c M_0^0}{\mu_R} + O(p), \quad \frac{1 + d_c M^*}{\mu^*}\bigg|_{p=\infty} = \frac{1 + (M_0^\infty + M_{-1}^\infty/p)d_c}{\mu_R + \mu_M} + O(1/p^2) \tag{22}$$

In turn, the series expansion of (12a) and (12b) read:

$$\frac{1 + Q^* d_c}{k_s^*}\bigg|_{p=0} = \frac{1 + Q_0^0 d_c}{k_R} + \theta(p), \quad \frac{1 + Q^* d_c}{k_s^*}\bigg|_{p=\infty} = \frac{1 + (Q_0^\infty + Q_{-1}^\infty/p)d_c}{k_R + k_M} + O(1/p^2), \tag{23}$$

$$\frac{1 + d_c M^*}{\mu^*}\bigg|_{p=0} = \frac{1 + d_c M_0^0}{\mu_R} + O(p), \quad \frac{1 + d_c M^*}{\mu^*}\bigg|_{p=\infty} = \frac{1 + (M_0^\infty + M_{-1}^\infty/p)d_c}{\mu_R + \mu_M} + O(1/p^2) \tag{24}$$

This allows the identification of six parameters (see (16)), where:

$$
Q_M^e = Q_e^\infty = \frac{4}{3} \frac{(k_R + k_M)(3k_R + 3k_M + 4\mu_R + 4\mu_M)}{(\mu_R + \mu_M)(3k_R + 3k_M + \mu_R + \mu_M)}, \quad Q_M^v = Q_0^0 = \frac{4}{3} \frac{k_M(3k_R + 4\mu_M)}{\mu_M(3k_R + \mu_M)},
$$

$$
Q_1^0 = \frac{2}{9} \frac{(9k_R^2 + 6k_R\mu_R + 4\mu_R^2)(-3k_R\eta_M^d + 2\mu_R\eta_M^s)}{9\mu_R^2(3k_R + \mu_R)^2}, \quad M_1^0 = \frac{8}{45} \frac{(63k_R^2 + 60k_R\mu_R + 16\mu_R^2)(3k_R\eta_M^d - 2\mu_R\eta_M^s)}{(9k_R^2 + 9k_R\mu_R + 2\mu_R^2)^2},
$$

$$
M_M^e = M_e^\infty = \frac{16}{45} \frac{(9k_R + 9k_M + 4\mu_R + 4\mu_M)}{(3k_R + 3k_M + \mu_R + \mu_M)} \frac{(3k_R + 3k_M + 4\mu_R + 4\mu_M)}{(3k_R + 3k_M + 2\mu_R + 2\mu_M)},
$$

$$
M_M^v = M_0^0 = \frac{16}{45} \frac{(3k_R + 4\mu_R)(9k_R + 4\mu_R)}{(9k_R^2 + 9k_R\mu_R + 2\mu_R^2)}
$$

$$(25)$$

Appendix B - Burgers model

The damaged stiffness and viscosity parameters (17) are determined by the developments in series of the estimated apparent modulus (15) to the first-order at p (and at 1/p) when p goes to zero (p goes to infinity) which could be equal to those indicated in (12a) and (12b), where:

$$
Q_M^e = Q_e^\infty = \frac{4}{3} \frac{k_M(3k_M + 4\mu_M)}{\mu_M(3k_M + \mu_M)}, \quad Q_M^v = Q_0^0 = \frac{16}{9} \frac{\eta_M^s(\eta_M^s + 2\eta_M^d)}{\eta_M^d(2\eta_M^s + \eta_M^d)},
$$

$$
Q_K^e = Q_0^0 + \frac{3k_K}{\eta_M^s} Q_1^0 - \frac{k_K}{k_M}(Q_0^\infty - Q_0^0), \quad Q_K^v = Q_0^\infty + \frac{\eta_K^s}{3k_M} Q_{-1}^\infty - \frac{\eta_K^s}{\eta_M^s}(Q_0^0 - Q_0^\infty),
$$

$$
Q_1^0 = \frac{32}{9} \frac{\eta_M^s}{\eta_M^d} \frac{({\eta_M^s}^2 + \eta_M^s\eta_M^d + {\eta_M^d}^2)}{(2\eta_M^s + \eta_M^d)^2} \left[\frac{\eta_M^s}{3} \left(\frac{1}{k_M} + \frac{1}{k_K} \right) - \frac{\eta_M^d}{2} \left(\frac{1}{\mu_M} + \frac{1}{\mu_K} \right) \right],
$$

$$
Q_{-1}^\infty = -\frac{4}{3} \frac{k_M}{\mu_M} \frac{(9k_M^2 + 6\mu_M k_M + 4\mu_M^2)}{(3k_M + \mu_M)^2} \left[3k_M \left(\frac{1}{\eta_M^s} + \frac{1}{\eta_K^s} \right) - 2\mu_M \left(\frac{1}{\eta_M^d} + \frac{1}{\eta_K^d} \right) \right]
$$

$$(26)$$

and:

$$
M_M^e = M_e^\infty = \frac{16}{45} \frac{(9k_M + 4\mu_M)}{(3k_M + \mu_M)} \frac{(3k_M + 4\mu_M)}{(3k_M + 2\mu_M)}, \quad M_M^v = M_0^0 = \frac{32}{45} \frac{(\eta_M^s + 2\eta_M^d)}{(\eta_M^s + \eta_M^d)} \frac{(3\eta_M^s + 2\eta_M^d)}{(2\eta_M^s + \eta_M^d)},
$$

$$
M_K^e = M_0^0 + \frac{2\mu_K}{\eta_M^d} M_1^0 - \frac{\mu_K}{\mu_M}(M_0^\infty - M_0^0), \quad M_K^v = M_0^\infty + \frac{\eta_K^d}{2\mu_M} M_{-1}^\infty - \frac{\eta_K^d}{\eta_M^d}(M_0^0 - M_0^\infty),
$$

$$
M_1^0 = \frac{32}{45} \frac{\eta_M^s\eta_M^d}{(\eta_M^s + \eta_M^d)^2} \frac{(7{\eta_M^s}^2 + 10\eta_M^s\eta_M^d + 4{\eta_M^d}^2)}{(2\eta_M^s + \eta_M^d)^2} \left[\frac{\eta_M^s}{3} \left(\frac{1}{k_M} + \frac{1}{k_K} \right) - \frac{\eta_M^d}{2} \left(\frac{1}{\mu_M} + \frac{1}{\mu_K} \right) \right],
$$

$$
M_{-1}^\infty = -\frac{16}{15} \frac{k_M\mu_M}{(3k_M + \mu_M)^2} \frac{(63k_M^2 + 60\mu_M k_M + 16\mu_M^2)}{(3k_M + 2\mu_M)^2} \left[3k_M \left(\frac{1}{\eta_M^s} + \frac{1}{\eta_K^s} \right) - 2\mu_M \left(\frac{1}{\eta_M^d} + \frac{1}{\eta_K^d} \right) \right]
$$

$$(27)$$